Available online at www.sciencedirect.com

ScienceDirect

Current Opinion in Biomedical Engineering

Biomechanics of cardiac development in zebrafish model

Tanveer Teranikar, Phuc Nguyen and Juhyun Lee

Abstract

Zebrafish (*Danio rerio*) larvae are emerging as high-throughput, chemical screening assays for investigating congenital cardiomyopathies. Despite distinct anatomical and genomic differences with humans, zebrafish share a conserved regulatory network of transcription factors modulating heart development with mammals. Consequently, external embryonic fertilization and optical transparency in conjunction with fluorescent reporters localizing endogenous proteins provide an ideal platform for studying molecular mechanisms underlying complex human heart development. In this regard, recent advances in light sheet microscopy (LSM) have enabled non-invasive, *in vivo* reconstruction of dynamic cardiac biomarkers during early stages of embryonic zebrafish heart development. In this review, we discuss the development of cardiovascular disease progression pipelines using zebrafish and LSM to identify genetic and molecular drivers of human cardiac disease.

Address

Joint Department of Bioengineering, UT Arlington, UT Southwestern Medical Center, Arlington, TX 76010, USA

Corresponding author: Lee, Juhyun (juhyun.lee@uta.edu)

Current Opinion in Biomedical Engineering 2023, **27:**100459

This review comes from a themed issue on **Biomechanics of growth and development**

Edited by **Tzung Hsiai**

For complete overview of the section, please refer the article collection - Biomechanics of growth and development

Received 26 August 2022, revised 21 March 2023, accepted 31 March 2023

https://doi.org/10.1016/j.cobme.2023.100459

Keywords

Zebrafish, Light sheet microscopy, Transgenic.

Introduction

Cardiovascular disease (CVD) has endured as the leading cause of mortality in US residents for nearly a century, since 1933 [1]. Furthermore, CVD has resulted in approximately 18 million deaths globally in 2020 [2–4]. Despite the development of novel diagnostic tools and therapies improving CVD prognosis over the last decade, CVD incidence remains prevalent in aging populations worldwide and is further exacerbated by exposure to contributory risk factors [1–3]. Furthermore, the complexity of molecular signaling pathways and modulation of cardiac output to renal and nervous systems result in the manifestation of CVD as a plethora of clinical pathologies [5]. Hence, there is a need for *bona fide* high throughput, *in vivo* modeling platforms to identify biomarkers associated with the disruption of cardiac output or biomechanical abnormalities [6,7].

Commonly occurring CVDs include hypertension, atherosclerosis, cardiomyopathies (hypertrophic, dilated, and non-compaction), congenital heart defects (CHD), and arrhythmia [2,3,8,9*]. Moreover, CVDs have been understood to alter cardiac mechanotransduction in the form of impaired blood flow, contractility, or hemodynamic shear stress [10,11]. Structural phenotypes of CVD include abnormal cardiac chamber size, shape, myocyte eccentricity, or defects in myocyte orientation to ventricular myocardial thickness [8,9*,12–14*]. As a result, accurate mutagenesis models are required for the effective clinical translation of pharmaceutical compounds [15].

Traditionally, higher-order animals such as canines, porcine, or sheep have been used to study tissue remodeling associated with human CVD/CHD and for therapeutic drug screening, due to conserved molecular, metabolic, hemodynamic, and *in vivo* cardiac biomechanics. However, large animal models pose several challenges, including the very high cost of infrastructure for animal husbandry, long breeding cycles, and the need for skilled technicians for complicated animal surgery [16]. These factors result in challenging study throughput and negatively impact clinical reproducibility [15,17,18]. Furthermore, the lack of transgenic models or gene editing tools capable of *in vivo* spatiotemporal genetic modulation limits the utility of large animals in validating developmental signaling pathways regulating progenitor cell fate or lineage-specific contributions [19].

In this regard, zebrafish are emerging as very high throughput and genetically tractable vertebrate models for replicating the developmental environment of disease progression in CVD pathophysiology [20]. Interestingly, despite exhibiting divergent or complementary characteristics, the zebrafish genome contains paralogous pairs of genes for every set of mammalian orthologs. Moreover, approximately 70% of human genes have at least one zebrafish ortholog. In this regard, a wide array

of gene editing tools has been developed to propagate modified contractile apparatus or CVD pathophysiology in multiple zebrafish generations, allowing to produce multiple, stable zebrafish generations for studying mutagenesis [21,22]. Forward genetic screens, which are aided by transposon-mediated mutagenesis, and reverse genetic screens, which involve gene targeting/ablation using morpholino-mediated gene knockdown or targeting induced local lesions (TILLING), have been developed [21]. In addition, transient gene overexpression is achieved through the injection of mRNA or DNA, and stable gene overexpression using transgenesis [21].

Other benefits of using zebrafish as model organisms include very high breeding capability (~100 embryos per cycle), ease of fluorescence transgene insertion into zebrafish genome, and conserved vasoconstrictor/dilator pharmaceutical drug response among others [7,21,23–25]. Moreover, optically transparent zebrafish embryos mature externally through passive oxygen and nutrient diffusion. These characteristics provide access to single-micron scale and sub-second frame rate *in vivo* image acquisition via Optical Sectioning Fluorescence Microscopy (OSM) [9*, 26].

Recent advances in opto-mechanics have resulted in the evolution of two-dimensional light microscopy into multidimensional [3d, 4d (3d + time)] OSM in the form of confocal and light sheet microscopes (LSM) [27–31]. Consequently, biologists have leveraged micron-scale spatial resolution and millisecond temporal resolution offered by OSM to reconstruct dynamic processes such as embryogenesis or angiogenesis in zebrafish with high throughput and reproducibility [26,32–34]. However, planar one-dimensional excitation of LSM has emerged as the preferred method over two-dimensional point scanning in confocal microscopes [35]. This is attributed to abilities such as sample acquisition in multiple views, integration of multiple emission channels, minimal photobleaching, and penetration depth in the order of millimeters without sacrificing spatiotemporal resolution [29,36,37*]. Furthermore, excitation strategies such as structured illumination microscopy (SIM) or axial/oblique sweeping LSM have enabled access to nanometer spatial resolution [29,38,39].

The objective of this review is to assess the suitability of zebrafish as an *in vivo* genetic toolbox and evaluate novel gene functions or phenotypic characterization of human CVD/CHD (Figure 2). Furthermore, the study aims to demonstrate the potential of LSM as an imaging toolbox for *in silico*, multidimensional reconstruction of *in vivo* cardiac morphogenesis and image-based signaling pathway study or biomechanics analysis in embryonic zebrafish.

Biomechanical modeling of cardiac phenotypes and genotypes

Two chambered zebrafish hearts exhibit unique structural differences with respect to a mammalian heart, such as the absence of chamber septation or a His-Purkinje system, besides the presence of a specialized outflow tract, i.e. bulbus arteriosus (BA) [8,9]*.

However, the zebrafish heart consists of myocardium and endocardium like other vertebrates, besides having orthologs with human CVD genes [8,9*, 39]. The well-annotated zebrafish genome has made it possible to characterize a wide array of phenotypes, such as abnormal cardiac function, valve morphology, chamber volume, or contractility phenotypes [9*, 11,40,41. Recent zebrafish imaging studies suggest that biomechanical cues are involved in deciding the cell fate of cardiac progenitor cells (CPCs) into specialized tissue, such as endothelium-derived mesenchymal cells for endocardial cushions or trabeculation [8,40,43]. Consequently, abnormalities in contractility, blood flow-induced shear forces, or mechanosensitive pathways result in embryonic lethality or cardiac malformations such as CHD's and cardiomyopathies [8–10] (Figure 1). In this regard, LSM has emerged as a powerful imaging modality for investigating zebrafish pathophysiology, due to ability to perform cellular scale 4d (3d + time) volumetric reconstruction at rapid frame rates.

Mechanical efficiency of developing zebrafish ventricle

Heart development begins with a peristaltic linear heart tube (LHT) at two days post-fertilization (dpf) that undergoes looping to form a morphologically separate atrium and ventricle at approximately 4 dpf [8,9[8,9*]. Any cardiac malformations during these developmental stages such as migration of mesodermal CPCs during peristaltic LHT formation, endocardial cushion formation, or myocardial compaction adversely affect the hemodynamic performance of embryonic heart [11,43]. Hence, there is a need to characterize the mechanical pumping efficiency of developing zebrafish heart.

Salehin et al. demonstrate the versatility of LSM modality by characterizing embryonic zebrafish ventricular pressure-volume (PV) loop and other cardiovascular phenotypes across 3–5 dpf, using the *Tg(cmlc2:mCherry;fli1a:GFP)* zebrafish lines [44**]. Optical sections were acquired in an orthogonal perspective to the camera to reconstruct ventricular volumes by sample translation through the static light sheet at discrete steps (2 um) using mechanical actuators [43]. Because of non-gated *in vivo* image acquisition, authors reconstructed dynamic ventricular volumes *a posteriori* by minimizing the error in the least squared intensity of adjacent optical sections. Authors highlight the implications of estimating the cardiac cycle period during 4d

Figure 1

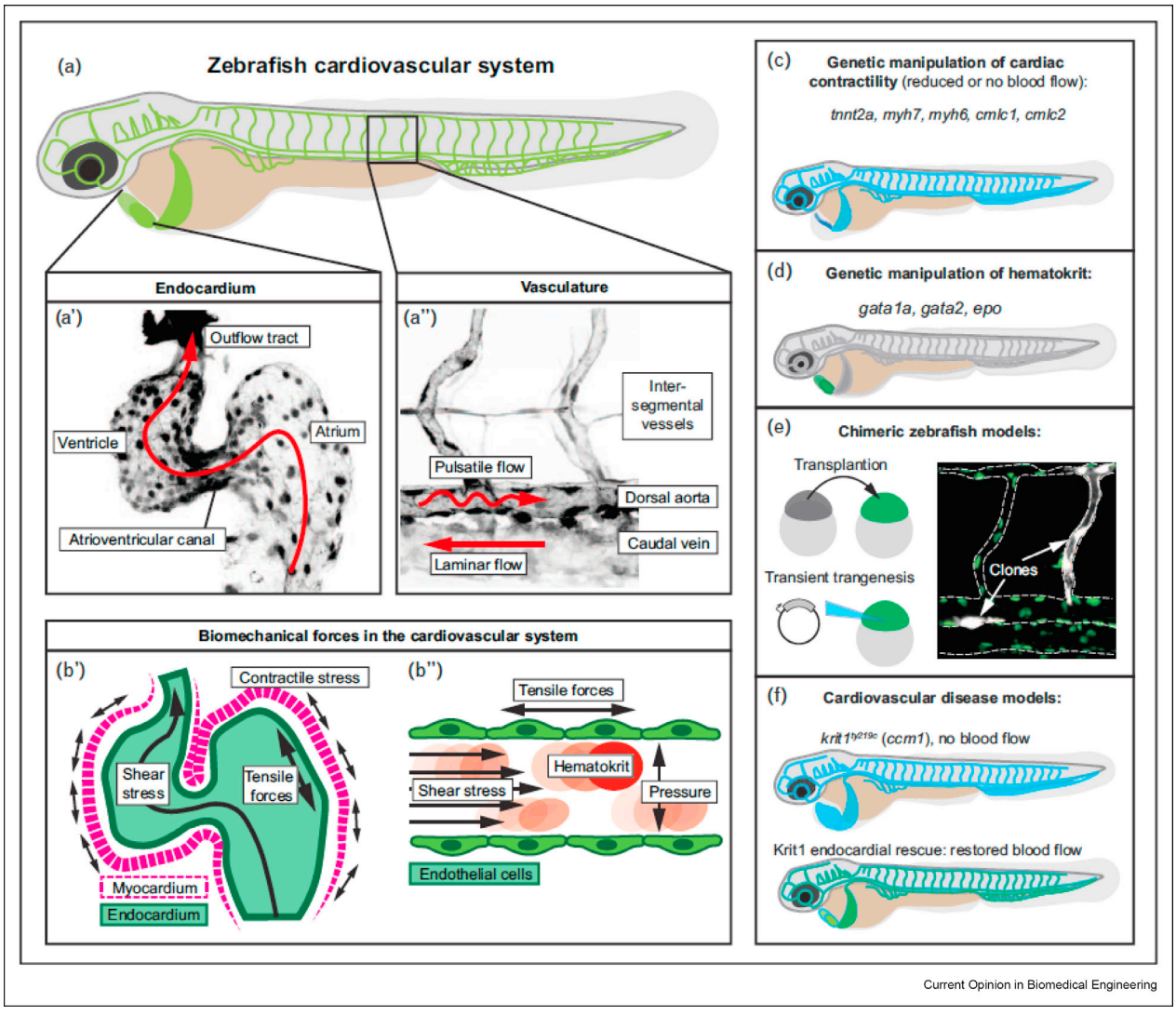

(a) Illustrative representation of the zebrafish cardiovascular system at 2 dpf. **(a')** Outflow tract (OFT), atrioventricular canal (AVC), ventricle, and atrium of the zebrafish endocardium. Red arrow represents flow-related forces through the chambers of the heart. **(a')** The zebrafish dorsal aorta experiences pulsatile flow-related forces, represented by the wavy-shaped red arrow. Flow-related forces through the caudal vein are laminar, represented by the straight red arrow. **(b')** Illustrative representation of contractile stress by the myocardium and fluid shear stress caused by blood flow. **(b")** Representation of fluid shear stress and pressure within the vasculature. **(c)** Transgenic zebrafish with removal of cardiac contractility genes results in reduction or even elimination of blood flow through blue vasculature region. **(d)** Genetic alteration of hematopoiesis genes, represented by grey vasculature region, results in changes in red blood cell quantities. **(e)** Representation of donor cell transplant into wildtype vasculature cells (grey cells → green cells, respectively). **(f)** Schematic of cerebral cavernous malformation (CCM) in the zebrafish heart. *Krit1(ccm1)* mutation causes heart defects and reduced blood flow, represented by blue vasculature region. Blood flow is restored through expression of *krit1* protein and variations in blood flow through blue-green vasculature region can be examined [11]. (For interpretation of the references to color in this figure legend, the reader is referred to the Web version of this article.)

(3d + time) synchronization to ensure neighboring image slices are in phase with the cardiac cycle. In this respect, acquiring multiple optical sections requires camera pixel exposure time (10 ms) reset. Intraventricular pressure measurements [peak systolic ventricular pressure (PSVP) and end-diastolic ventricular pressure (EDVP)] were acquired using a standalone servo-null micropressure system. An offset in electrical resistance of a pre-calibrated borosilicate-tipped glass electrode was recorded with respect to variation in ventricular pressure. mCherry-labeled myocardial volume was used for the separation of endocardial boundary from ventricular blood volume. The region-of-interest (ROI) confined within GFP-labeled ventricular endocardium was reconstructed for calculating end-systolic volume (ESV), end-diastolic volume (EDV),

stroke volume (SV = EDV − ESV), stroke work (SW = $\oint p.d$ (vol)), ejection fraction (EF = EDV − ESV/EDV), and cardiac output [CO = SV x heart rate (HR)]. In addition, authors demonstrate the time derivative of ventricular volume as a surrogate for ventricular blood flow rate, enabling the characterization of cardiac chamber driving potential or impedance to blood influx.

Authors reported a 50% increase in PSVP from 7.52 ± 0.77 mmHg at 3 dpf to 11.26 ± 1.31 mmHg at 5 dpf, with a 3% decrease in EDVP from 1.36 ± 0.52 mmHg to 1.32 ± 0.19 mmHg. ESV was found to increase from 0.08 ± 0.01 nL at 3 dpf to 0.18 ± 0.01 nL at 5 dpf, along with an increase in EDV from 0.18 ± 0.02 nL from 3 dpf to 0.40 ± 0.03 nL at 5 dpf. Authors also reported 23% increase in HR from 112.87 ± 8.58 beats/min to 139.16 ± 6.70 beats/min, along with a 178% increase in CO from 10.5 ± 0.6 nL/min to 29.1 ± 2.18 nL/min across 3 to 5 dpf, respectively. SW was also observed to increase 222% from 0.062± 0.008 nJ at 3 dpf to 0.200 ± 0.023 nJ at 5 dpf. Thus, the

Figure 2

Transgenic zebrafish line	Embryonic zebrafish developmental stage [days post fertilization (dpf)]	Phenotype of transgenes and study performed
Tg (cmlc2: mCherry; fli1a: GFP)	2 dpf (primitive cardiac valve formation) – 5 dpf (cardiac trabeculation and complete chamber development)	GFP fluorescence localized in endothelial cells lining the blood vessels and heart and mCherry fluorescence localized in myocardial heart muscle, was acquired to quantify intra-ventricular pressure, ventricular volume, stroke volume, ejection fraction, cardiac output, and blood flow rate.
Tg (fli1a: GFP)	2 dpf (primitive cardiac valve formation) – 5 dpf (cardiac trabeculation and complete chamber development)	The GFP signal detected in endothelial cells, allowing for the assessment of ventricular strain and ejection fraction.
Tg (tp1: GFP)	2 dpf (primitive cardiac valve formation) – 5 dpf (cardiac trabeculation and complete chamber development)	The GFP signal was observed in cells that contained activated Tp1 promoter with Notch-responsive elements, enabling the investigation of the role of Notch1b in regulating VB valve morphogenesis through contractile force.
Tg (cmlc2: GFPnuc)	2 dpf (primitive cardiac valve formation) – 5 dpf (cardiac trabeculation and complete chamber development)	The GFP signal was localized on cardiomyocyte nuclei. Thus, ventricular contractility, ventricular myocardial nuclei count, area and eccentricity were measured. .

Current Opinion in Biomedical Engineering

Transgenic zebrafish (*Danio rerio*) models are used for creating forward genetics human CVD/CHD phenotypic screens.

imaging study demonstrates the utility of LSM for quantifying hemodynamic parameters *in vivo* across distinct developmental stages of zebrafish cardiogenesis (LHT at 24 dpf with no valve formation to the specification of atrium, ventricle, and valve leaflets at ~ 96–120 dpf) [44**].

In this regard, Salehin et al. describe the significance of having the ability to synchronize discrete hemodynamic parameters to interpolate global CO, as well as consequently assess phenotypes that are exhibited in CVD [44**]. This is often complicated by the small size of the zebrafish (~4 mm). The synchronization of intraventricular pressure and ventricular volume was achieved by identifying distinct events in the cardiac cycle and matching in time. Isovolumic relaxation and end diastole were used for AV valve opening and closing, and the start and end of ejection were marked by the opening and closing of ventriculobulbar (VB) valve. Hence, improvement in mechanical function during embryonic heart development is attributed to increasingly efficient hemodynamic parameters due to valve leaflet formation from endocardial cushions [11,39,43].

Effect of contractility and fluid flow on valve formation

While cardiomyocyte or valve maturation contributes to improvement in the pumping efficiency of embryonic zebrafish, mechanosensitive signaling pathways are hypothesized to regulate valvulogenesis [10]. Hsu et al. sought to investigate the effect of ventricular contractility and fluid flow-induced shear stress on endocardial–mesenchymal transition (EndoMT) in AV and VB valve formation [43] (Figure 3). Authors demonstrate the utility of the zebrafish animal model as a genetic toolkit and 4d (3d + time) LSM as an *in vivo* dynamic volume acquisition toolkit [11,43]. Pharmacological modulation of zebrafish ventricular contractility and HR using a nonselective β-receptor agonist (isoproterenol hydrochloride, (increase)), selective β1-receptor antagonist (metoprolol tartrate, (reduction)), or BDM ((2,3-butanedione monoxime [BDM] was performed. In addition, blood viscosity and hematopoiesis were downregulated by microinjections of *Gata1a* morpholino oligonucleotide (MO), while *EPO* mRNA upregulated viscosity. Furthermore, *Tnnt2a* MO was administered for arresting atrial and ventricular contractility, while *Plcγ1*MOs were used for inhibition

Figure 3

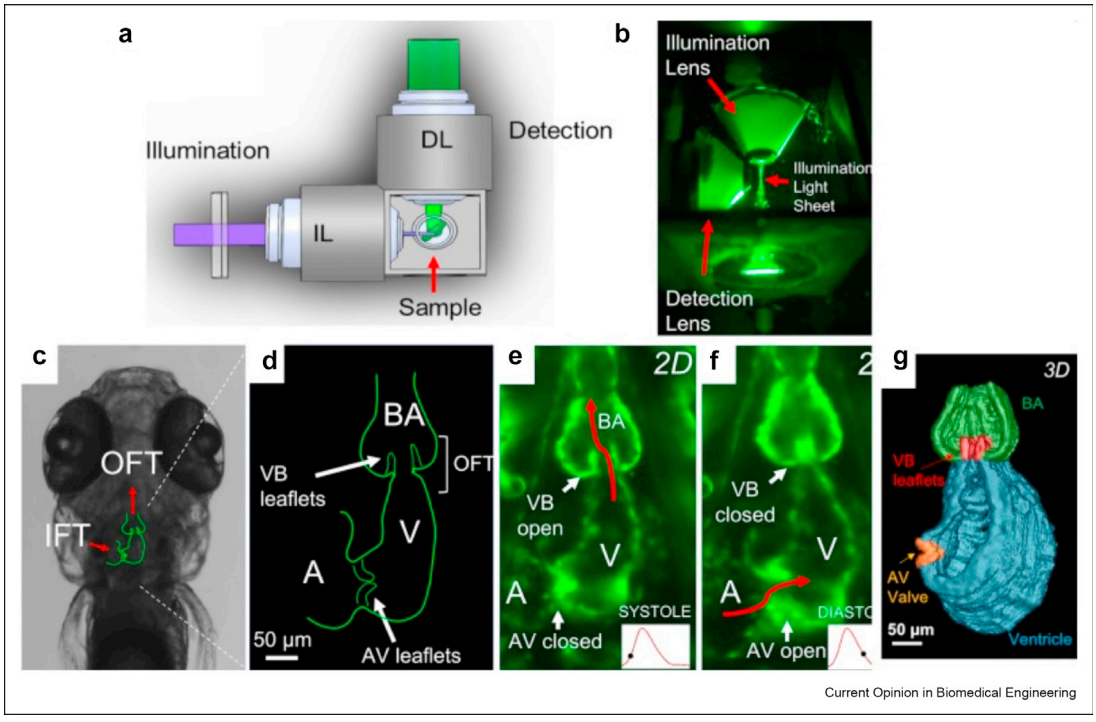

Orthogonal optical pathway for single-sided illumination and dual detection represented as **(a)** a schematic diagram and **(b)** a photograph. **(c)** Bright-field image of a 5 dpf zebrafish, with heart outlined in green and inflow tract (IFT) and outflow tract (OFT) represented with red arrows. **(d)** Schematic of heart depicting AV and VB valve leaflets, atrium (A), ventricle (V), OFT, and BA. **(e)** Light-sheet fluorescence microscopy (LSFM) image of 5 dpf heart during systole with VB valve open. **(f)** LSFM image of 5 dpf heart during diastole with AV valve open. **(g)** The heart during systole, represented as a 3D reconstruction with the VB valve in red and AV valve in orange [43]. (For interpretation of the references to color in this figure legend, the reader is referred to the Web version of this article.)

of ventricular contractility only. Authors relied on the well-annotated zebrafish genome for visualizing varying effects of genetic manipulations. *Tg*(*fli1a: GFP*) line was used for endothelial and endocardial cells, *Tg(gata1:dsRed)* for red blood cells, *Tg(tp1:GFP)* for reporting Notch1 activity, and *Tg(cmlc:mCherry)* for reconstruction myocardial cardiomyocytes and *cloche* zebrafish mutants with lacking endocardium. Authors report upregulation of myocardial contractility and hemodynamic wall shear stress (WSS) using isoproterenol cause enlarged, abnormal valve leaflets, whereas the inhibition of contractility using BDM, *Tnnt2a*, or *Plcγ1*MOs led to the absence of AV and VB valves. Interestingly, metoprolol vs control zebrafish line did not result in any significant abnormalities due to conserved myocardial contractility and *Notch1b* signaling. Similarly, pharmaceutical modulation of blood viscosity using EPO mRNA resulted in enlarged leaflets for increased viscosity and WSS. On the other hand, no significant effect on *Notch1b* signaling and valve structures was observed for *Gata1a* MO microinjection.

The imaging group relied on SV and EF for contractility analysis in conjunction with blood velocity and time-averaged wall shear stress (TAWSS) for hemodynamic analysis. Dynamic blood flow simulation required endocardial boundary segmentation using intensity-based thresholding. Edges of binarized images were deformed according to *in vivo* endocardial groove and ridge topology using level set advection techniques and finally converted into a triangulated surface mesh for computational fluid domain (CFD) analysis. Moreover, authors relied on minimizing an intensity-based non-rigid deformable objective function based on $\mathbf{E}_{obj} = \mathbf{E}_{sim}(I(\mathbf{x}), J(\tau(\mathbf{x}))) + \lambda\mathbf{E}_{reg}(\tau(\mathbf{x}))$ for ensuring synchronized optical sections across the cardiac cycle. Briefly, the sum of squared differences (SSD) similarity function was used for calculating $\mathbf{E}_{sim}$ and free-form transformation deformation model (FFD) based on cubic B splines for mapping endocardial ROI across different parts of the cardiac cycle. The squared norm of the FFD transformation gradient ($\mathbf{E}_{reg} = {}^{1}/_{2}\ \|\nabla\tau(\mathbf{x})\|^2$ was used for controlling the degree of deformation. Authors relied on interface tracking arbitrary Lagrangian−Eulerian (ALE) methods for tracking endocardial displacement and blood domain within ventricular endocardial cavity. The endocardial wall velocity was computed using the deformation map obtained during image registration.

Furthermore, the imaging group observed upregulation of mechanotransducive *Notch1b* signaling pathway by administering isoproterenol and EPO mRNA led to valve hyperplasia, and downregulation by administering BDM, *Tnnt2a,* or *Plcγ1*MO's led to valve hypoplasia. To investigate the impact of biomechanical transduction on EndoMT, the Hsu et al. utilized immunostaining against DM-GRASP, a mesenchymal marker, to quantify cell count and volume of VB valve. This allowed them to elucidate the effect of biomechanical force-mediated Notch1b activity on valve cells. By administering isoproterenol and EPO mRNA, which increased myocardial contractility and TAWSS, the authors observed an increase in DM-GRASP + cells using *Tg(cmlc2: mcherry)* to visualize the VB valvular regions, as *cmlc2 (cardio myosin light chain 2)* highlights myocardium. Interestingly, an increase in WSS led to a slightly larger volume of cell adhesion molecules. Conversely, when contractility was attenuated with BDM, no DM-GRASP + cells were observed in the VB canal region.

Hence, authors conclude the inhibition of contractility to be primarily responsible for abnormal valve leaflet maturation or hyperplasia [43]. However, coordination with shear stress, blood velocity, and mechanotransducive *Notch1b* is required for the initiation and remodeling of endocardial cushions into mature valves [10,40,43]. Hence, the imaging study highlights the dynamic spatiotemporal resolution of LSM modality for the reconstruction of fluid flow environment or other biomechanical cues using non-ionizing, non-gated LSM optical sectioning.

Effect of contractility on cardiomyocyte morphology

Specification of CPCs into diverse cardiac lineages has been observed to be regulated by local blood flow velocity and contractility, as described in previous sections [9*, 13*, 39,42,43. This is evident by abnormal valve growth because of impaired blood flow or improper crosstalk between signaling pathways in AVC or outflow (OFT) tract [40,43]. Hence, in addition to mechanical properties, it is essential to characterize dynamic cardiac cell deformation in response to blood flow and contractile forces [13*, 45**].

Teranikar et al. demonstrate the use of *Tg(cmlc:GFPnuc)* zebrafish line for quantifying ventricular contractility across 2−5 dpf using non-gated *in vivo* image acquisition as discussed previously [13*, 45**] (Figure 4). Furthermore, authors were able to characterize dynamic change in nuclei eccentricity and volume across the cardiac cycle. Furthermore, ventricular myocardial nuclei were quantified through several phases of embryonic development. At 2, 3, 4, and 5 dpf, nuclei count was observed to be 159 ± 13, 222 ± 17, 260 ± 13, and 284 ± 10, respectively, indicating ventricular maturation as observed by increasing hemodynamic efficiency in previous sections. Analysis of the innermost curvature (IC) and outermost curvature (OC) ventricular regions as a function of time revealed that the OC region has a greater area ratio than IC. Moreover, the volumes of OC nuclei during systole and diastole were larger than that of the nuclei within the IC region. In addition to greater

Figure 4

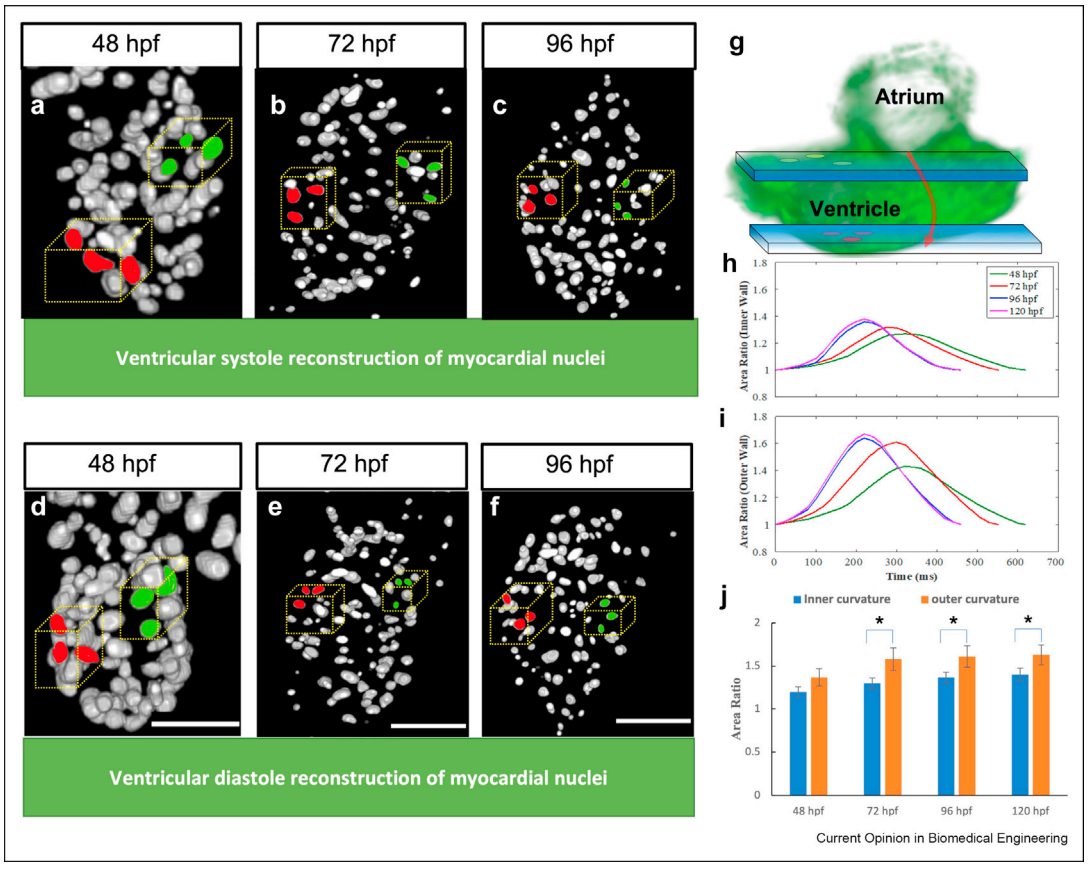

Reconstruction of ventricular myocytes during systole at **(a)** 2 dpf, **(b)** 3 dpf, and **(c)** 4 dpf, as well as during diastole at **(d)** 2 dpf, **(e)** 3 dpf, and **(f)** 4 dpf. **(g)** Illustrative representation of ventricular nuclei sampling in the region of interest. *Green markers: Innermost curvature contractility. Red markers: Outermost curvature contractility. Blue windows: Light sheet sections.* **(h)** Area ratio for innermost curvature at 2, 3, 4, and 5 dpf was found by tracking three cardiomyocytes as indicated in green in panel G, which demonstrate increasing contractility as development progresses. **(i)** Area ratio for outermost curvature at 2, 3, 4, and 5 dpf was found by tracking three cardiomyocytes as indicated in red in panel G, which show more pronounced contractility compared to innermost curvature. **(j)** Starting at 3 dpf, the outermost curvature has significantly higher area ratio than innermost curvature *(n=3, p=0.05, one-tailed t-test)* [13]. (For interpretation of the references to color in this figure legend, the reader is referred to the Web version of this article.)

volume, the OC nuclei were found to have a more ellipsoid morphology, averaging a 0.71 elongation index. Cardiomyocyte nuclei in the IC, on the other hand, displayed a smaller, spherical morphologies with an average elongation index of 0.91.

The data from this study suggest that cardiomyocyte nuclei deformation is unique to different regions of the ventricle and is dependent upon the amount of mechanical exertion experienced in those regions. While previous sections relied on tracking blood flow domain for quantifying hemodynamic forces, this study focuses on tracking dynamic cardiomyocyte nuclei across the cardiac cycle. Authors relied on the area ratio to represent ventricular deformation between selected nuclei markers. The study hypothesizes that larger, elongated nuclei volumes on the outermost curvature are due to direct blood flow from AVC and higher area ratio in comparison to spherical nuclei in the inner curvature [13*].

This study illustrates the viability of the zebrafish heart as a model for contractility-mediated morphology, as well as the efficacy of LSM for imaging at the nuclear level.

Conclusion

The zebrafish has become an increasingly popular vertebrate model for studying human CVD's, due to low cost, convenient animal husbandry, and ability to rapidly screen novel therapeutic compounds. Furthermore, advancements in whole genome modification techniques have made it possible to generate stable transgenic or mutant zebrafish models that closely mimic the developmental environment of human CVD/CHD. This has allowed researchers to study the effects of specific

genetic mutations or environmental factors more accurately on disease development and progression.

Overall, the review highlights the synergistic effect of LSM in analyzing biomechanics of dynamic fluorescent signals within embryonic zebrafish. The fluorescence modality's ability to optically section fluorescent biomarkers at millimeter penetration depth with high spatiotemporal resolution has pushed the boundaries in elucidating developmental biomechanical cues *in vivo*. In addition, minimal phototoxicity, ability to perform time-lapse imaging from multiple perspectives, and rapid volume acquisition (in milliseconds) with cellular resolution have enabled the characterization of cardiogenesis from cellular to organ level. As a result, LSM in conjunction with zebrafish models has great potential as an automated, multi-dimensional pipeline for facilitating the clinical translation of developmental biomarkers to higher-level animal models.

Funding

This study was supported by grants from AHA 18CDA34110150 (J.L.) and NSF 1936519 (J.L.).

Declaration of competing interest

The authors declare the following financial interests/personal relationships which may be considered as potential competing interests: Juhyun Lee reports financial support was provided by American Heart Association. Juhyun Lee reports financial support was provided by National Science Foundation.

Data availability

No data was used for the research described in the article.

Acknowledgements

We are sincerely grateful for AHA and NSF for supporting our work, and our lab peers for their consistent motivation.

References

Papers of particular interest, published within the period of review, have been highlighted as:

* of special interest
** of outstanding interest

1. Ritchey MD, Wall HK, George MG, Wright JS: **US trends in premature heart disease mortality over the past 50 years: where do we go from here?** *Trends Cardiovasc Med* 2020, **30**:364–374. https://doi.org/10.1016/j.tcm.2019.09.005.

2. Virani SS, Alonso A, Benjamin EJ, *et al.*: **Heart disease and stroke statistics—2020 update: a report from the American heart association**. *Circulation* 2020, **141**:e139–e596. https://doi.org/10.1161/CIR.0000000000000757.

3. Tsao CW, Aday AW, Almarzooq ZI, *et al.*: **Heart disease and stroke statistics—2022 update: a report from the American heart association**. *Circulation* 2022, **145**:e153–e639. https://doi.org/10.1161/CIR.0000000000001052.

4. Giardoglou P, Beis D: **On zebrafish disease models and matters of the heart**. *Biomedicines* 2019, **7**:15. https://doi.org/10.3390/biomedicines7010015.

5. Gut P, Reischauer S, Stainier DYR, Arnaout R: **Little fish, big data: zebrafish as a model for cardiovascular and metabolic disease**. *Physiol Rev* 2017, **97**:889–938. https://doi.org/10.1152/physrev.00038.2016.

6. Francoeur N, Sen R: **Advances in cardiac development and regeneration using zebrafish as a model system for high-throughput research**. *J Dev Biol* 2021, **9**. https://doi.org/10.3390/jdb9040040.

7. Fuentes R, Letelier J, Tajer B, Valdivia LE, Mullins MC: **Fishing forward and reverse: advances in zebrafish phenomics**. *Mech Dev* 2018, **154**:296–308. https://doi.org/10.1016/j.mod.2018.08.007.

8. Ding Y, Bu H, Xu X: **Modeling inherited cardiomyopathies in adult zebrafish for precision medicine**. *Front Physiol* 2020, **11**:599244. https://doi.org/10.3389/fphys.2020.599244. 599244.

9. * Bowley G, Kugler E, Wilkinson R, *et al.*: **Zebrafish as a tractable model of human cardiovascular disease**. *Br J Pharmacol* 2022, **179**:900–917. https://doi.org/10.1111/bph.15473.
Review exhaustively summarizes genetic or pharmacological *in vivo* modulation of transgenic zebrafish models, relevant to cardiovascular disease progression and heart regeneration.

10. Li R, Baek KI, Chang CC, Zhou B, Hsiai TK: **Mechanosensitive pathways involved in cardiovascular development and homeostasis in zebrafish**. *J Vasc Res* 2019, **56**:273–283. https://doi.org/10.1159/000501883.

11. Rödel C, Abdelilah-Seyfried S: **A zebrafish toolbox for biomechanical signaling in cardiovascular development and disease**. *Curr Opin Hematol* 2021. https://doi.org/10.1097/MOH.0000000000000648. Publish Ahead of Print.

12. Lee SE, Nguyen C, Yoon J, *et al.*: **Three-dimensional cardiomyocytes structure revealed by diffusion tensor imaging and its validation using a tissue-clearing technique**. *Sci Rep* 2018, **8**:6640. https://doi.org/10.1038/s41598-018-24622-6.

13. * Teranikar T, Villarreal C, Salehin N, *et al.*: **Scale space detector for analyzing spatiotemporal ventricular contractility and nuclear morphogenesis in zebrafish**. *iScience* 2022, **25**, 104876. https://doi.org/10.1016/j.isci.2022.104876.
Using transgenic zebrafish with myocardial nuclei specific fluorescence in conjunction with Light sheet microscopy, authors established a novel multi-dimensional, automated *in vivo* pipeline for quantifying chamber contractility and cell morphogenesis during embryonic heart development across the entire cardiac cycle.

14. * Kula-Alwar D, Marber MS, Hughes SM, Hinits Y: **Mef2c factors are required for early but not late addition of cardiomyocytes to the ventricle**. *Dev Biol* 2021, **470**:95–107. https://doi.org/10.1016/j.ydbio.2020.11.008.
Using transgenic zebrafish with myocardium specific fluorescence, authors developed a high throughput, chemical screening assay to quantify cardiomyocyte differentiation and proliferation from cardiac progenitors, responsible for modulation of cardiac chamber development and trabeculation.

15. Savoji H, Mohammadi MH, Rafatian N, *et al.*: **Cardiovascular disease models: a game changing paradigm in drug discovery and screening**. *Biomaterials* 2019, **198**:3–26. https://doi.org/10.1016/j.biomaterials.2018.09.036.

16. Shin HS, Shin HH, Shudo Y: **Current status and limitations of myocardial infarction large animal models in cardiovascular translational research**. *Front Bioeng Biotechnol* 2021, **9**:673683. https://doi.org/10.3389/fbioe.2021.673683. 673683.

17. Vyas MV, Gros R, Hackam DG: **Translation of cardiovascular animal models to human randomized trials**. *Am J Cardiol* 2020, **137**:141. https://doi.org/10.1016/j.amjcard.2020.10.027.

18. Silva Kleiton Augusto Santos, Emter Craig A: **Large animal models of heart failure**. *JACC (J Am Coll Cardiol): Basic to Translational Science* 2020, **5**:840–856. https://doi.org/10.1016/j.jacbts.2020.04.011.

19. Jorba I, Mostert D, Hermans LHL, van der Pol A, Kurniawan NA, Bouten CVC: **Vitro methods to model cardiac mechanobiology in health and disease**. *Tissue Eng C Methods* 2021, **27**(3): 139–151. https://doi.org/10.1089/ten.tec.2020.0342.

20. Dubey A, Ghosh NS, Singh R: **Zebrafish as an emerging model: an important testing platform for biomedical science**. *J Pharm Negat Results* 2022, **13**:2.

21. Rafferty SA, Quinn TA: **A beginner's guide to understanding and implementing the genetic modification of zebrafish**. *Prog Biophys Mol Biol* 2018, **138**:3–19. https://doi.org/10.1016/j.pbiomolbio.2018.07.005.

22. Adhish M, Manjubala I: *Effectiveness of zebrafish models in understanding human diseases—a review of models*. Heliyon; 2023. Published online.

23. Scholpp S: **Introduction: in vivo cell biology in zebrafish**. *Histochem Cell Biol* 2020, **154**:457–461. https://doi.org/10.1007/s00418-020-01931-4.

24. Santoro MM, Beltrame M, Panáková D, *et al.*: **Advantages and challenges of cardiovascular and lymphatic studies in zebrafish research**. *Front Cell Dev Biol* 2019, **7**:89. https://doi.org/10.3389/fcell.2019.00089. 89.

25. Crilly S, McMahon E, Kasher PR: **Zebrafish for modeling stroke and their applicability for drug discovery and development**. *null* 2022, **17**:559–568. https://doi.org/10.1080/17460441.2022.2072828.

26. Teranikar T, Messerschmidt V, Lim J, *et al.*: **Correcting anisotropic intensity in light sheet images using dehazing and image morphology**. *APL Bioeng* 2020, **4**:36103. https://doi.org/10.1063/1.5144613. 036103.

27. Poola PK, Afzal MI, Yoo Y, Kim KH, Chung E: **Light sheet microscopy for histopathology applications**. *Biomed Eng Lett* 2019, **9**:279–291. https://doi.org/10.1007/s13534-019-00122-y.

28. Elliott AD: **Confocal microscopy: principles and modern practices**. *Curr Protoc Cytom* 2020, **92**:e68. https://doi.org/10.1002/cpcy.68. e68.

29. Teranikar T, Lim J, Ijaseun T, Lee J: **Development of planar illumination strategies for solving mysteries in the subcellular realm**. *Int J Mol Sci* 2022, **23**. https://doi.org/10.3390/ijms23031643.

30. Chatterjee K, Pratiwi FW, Wu FCM, Chen P, Chen BC: **Recent progress in light sheet microscopy for biological applications**. *Appl Spectrosc* 2018, **72**:1137–1169. https://doi.org/10.1177/0003702818778851.

31. Peng Fei, Nie Jun, Lee Juhyun, *et al.*: **Subvoxel light-sheet microscopy for high-resolution high-throughput volumetric imaging of large biomedical specimens**. *Advanced Photonics* 2019, **1**, 016002. https://doi.org/10.1117/1.AP.1.1.016002.

32. Chakraborty T, Driscoll MK, Jeffery E, *et al.*: **Light-sheet microscopy of cleared tissues with isotropic, subcellular resolution**. *Nat Methods* 2019, **16**:1109–1113. https://doi.org/10.1038/s41592-019-0615-4.

33. Sapoznik E, Chang BJ, Huh J, *et al.*. In Lakadamyali M, Akhmanova A, Power R. *A versatile oblique plane microscope for large-scale and high-resolution imaging of subcellular dynamics*, **9**; 2020, e57681. https://doi.org/10.7554/eLife.57681. eLife.

34. Lee J, Vedula V, Baek KI, *et al.*: **Spatial and temporal variations in hemodynamic forces initiate cardiac trabeculation**. *JCI Insight* 2018, **3**, e96672. https://doi.org/10.1172/jci.insight.96672.

35. Ding Y, Lee J, Hsu JJ, *et al.*: **Light-sheet imaging to elucidate cardiovascular injury and repair**. *Curr Cardiol Rep* 2018, **20**:35. https://doi.org/10.1007/s11886-018-0979-6.

36. Wan Y, McDole K, Keller PJ: **Light-sheet microscopy and its potential for understanding developmental processes**. *Annu Rev Cell Dev Biol* 2019, **35**:655–681.

37. * Stelzer EHK, Strobl F, Chang BJ, *et al.*: **Light sheet fluorescence microscopy**. *Nature Reviews Methods Primers* 2021, **1**: 73. https://doi.org/10.1038/s43586-021-00069-4.
The review comprehensively summarizes configuration of Light sheet modality, for *in vivo* volumetric acquisition of vertebrate/invertebrate animal models, multi-dimensional cell cultures and multicellular organisms with high patio-temporal resolution.

38. Chang BJ, Dean KM, Fiolka R: **Systematic and quantitative comparison of lattice and Gaussian light-sheets**. *Opt Express* 2020, **28**(18):27052–27077. https://doi.org/10.1364/OE.400164.

39. Wu Y, Shroff H: **Faster, sharper, and deeper: structured illumination microscopy for biological imaging**. *Nat Methods* 2018, **15**:1011–1019. https://doi.org/10.1038/s41592-018-0211-z.

40. Dye B, Lincoln J: **The endocardium and heart valves**. *Cold Spring Harbor Perspect Biol* 2020, **12**:a036723. https://doi.org/10.1101/cshperspect.a036723.

41. Choe CP, Choi SY, Kee Y, *et al.*: **Transgenic fluorescent zebrafish lines that have revolutionized biomedical research**. *Laboratory Animal Research* 2021, **37**:26. https://doi.org/10.1186/s42826-021-00103-2.

42. Zhao MT, Ye S, Su J, Garg V: **Cardiomyocyte proliferation and maturation: two sides of the same coin for heart regeneration**. *Front Cell Dev Biol* 2020, **8**. https://doi.org/10.3389/fcell.2020.594226.

43. Hsu JJ, Vedula V, Baek KI, *et al.*: **Contractile and hemodynamic forces coordinate Notch1b-mediated outflow tract valve formation**. *JCI Insight* 2019, **5**, e124460. https://doi.org/10.1172/jci.insight.124460.

44. ** Salehin N, Villarreal C, Teranikar T, Dubansky B, Lee J, Chuong CJ: **Assessing pressure–volume relationship in developing heart of zebrafish in-vivo**. *Ann Biomed Eng* 2021, **49**:2080–2093. https://doi.org/10.1007/s10439-021-02731-0.
Authors developed a stable transgenic zebrafish model for quantifying developmental hemodynamic parameters i*n vivo,* by crossbreeding myocardial and endothelial specific fluorescence zebrafishes. In addition, authors integrated Light sheet microscopy image cardiac volumes with standalone servo null micro pressure system, for novel quantification of *in vivo* Pressure-Volume loop in zebrafish model.

45. ** Salehin N, Teranikar T, Lee J, Chuong C: **Ventricular anisotropic deformation and contractile function of the developing heart of zebrafish in vivo**. *Dev Dynam* 2023, **252**: 247–262.
By using transgenic zebrafish with myocardium specific fluorescence in conjunction with Light sheet microscopy, authors developed a multi-dimensional, automated *in vivo* pipeline for quantifying anisotropic cardiac chamber stiffness and deformation across the cardiac cycle, from development of linear heart tube to trabeculation.